EUROPEAN ORGANIZATION FOR NUCLEAR RESEARCH (CERN)

CERN-EP-2021-255
LHCb-PAPER-2021-036
21 July 2022

Constraints on the CKM angle γ from $B^{\pm} \to Dh^{\pm}$ decays using $D \to h^{\pm}h'^{\mp}\pi^0$ final states

LHCb collaboration[†]

This paper is dedicated to our friend and colleague Bernhard Spaan.

Abstract

A data sample collected with the LHCb detector corresponding to an integrated luminosity of 9 fb^{-1} is used to measure eleven *CP* violation observables in $B^{\pm} \to Dh^{\pm}$ decays, where h is either a kaon or a pion. The neutral D meson decay is reconstructed in the three-body final states: $K^{\pm}\pi^{\mp}\pi^0$; $\pi^+\pi^-\pi^0$; $K^+K^-\pi^0$ and the suppressed $\pi^{\pm}K^{\mp}\pi^0$ combination. The mode where a large *CP* asymmetry is expected, $B^{\pm} \to [\pi^{\pm}K^{\mp}\pi^0]_D K^{\pm}$, is observed with a significance greater than seven standard deviations. The ratio of the partial width of this mode relative to that of the favoured mode, $B^{\pm} \to [K^{\pm}\pi^{\mp}\pi^0]_D K^{\pm}$, is $R_{\mathrm{ADS}(K)} = (1.27 \pm 0.16 \pm 0.02) \times 10^{-2}$. Evidence for a large *CP* asymmetry is also seen: $A_{\mathrm{ADS}(K)} = -0.38 \pm 0.12 \pm 0.02$. Constraints on the CKM angle γ are calculated from the eleven reported observables.

Published in JHEP 07 (2022) 099

[†]Authors are listed at the end of this paper.

1 Introduction

Precision measurements of the Cabibbo-Kobayashi-Maskawa (CKM) unitarity triangle parameters are essential in the search for new physics in the quark flavour sector. The unitarity triangle can be overconstrained by measuring its three angles and two lengths. The angle $\gamma \equiv \arg(-V_{ud}V_{ub}^*/V_{cd}V_{cb}^*)$, where V_{ik} are the CKM matrix elements, is an ideal Standard Model benchmark since it is independent of top-quark couplings. It can be determined from measurements of *CP* violation in decays that are dominated by tree-level contributions with negligible theoretical uncertainties [1]. The world-average value, $\gamma = (66.2^{+3.4}_{-3.6})^\circ$ [2], is in good agreement with the value inferred from a global CKM fit where direct γ determinations are excluded: $\gamma = (65.5^{+1.1}_{-2.7})^\circ$ [3]. To test this agreement at the sub-degree level, it is important to develop new modes to complement established techniques.

The angle γ is the relative weak phase between $b \to c\bar{u}s$ and $b \to u\bar{c}s$ quark transition amplitudes. These transitions mediate the decays $B^- \to D^0K^-$ and $B^- \to \overline{D}^0K^-$, respectively.[1] By studying final states accessible to both D^0 and $\overline{D}^0$ mesons, phase information can be determined from the interference of the two amplitudes. As well as γ, the ratio of the magnitudes of the $B^- \to \overline{D}^0K^-$ to $B^- \to D^0K^-$ amplitudes, $r_B \approx 0.1$, and the relative strong phase, δ_B, determine the size of the interference. Such interference also occurs in $B^- \to D\pi^-$ decays, albeit with lower γ sensitivity due to additional Cabibbo suppression that leaves the amplitude ratio around 20 times smaller than for $B^- \to DK^-$ decays. Here D represents an admixture of the D^0 and $\overline{D}^0$ states.

The measurement of γ through $B^- \to DK^-$ decays was first suggested by Gronau, London & Wyler for D decays reconstructed in *CP* eigenstates; they are often referred to as GLW modes [4, 5]. The method was generalised by Atwood, Dunietz & Soni (ADS) to include non-charge-conjugate states [6, 7]. In ADS modes, the favoured (suppressed) $B^- \to Dh^-$ decay is followed by a suppressed (favoured) D meson decay, which has the effect of roughly balancing the two competing amplitudes, maximising their interference and thus their sensitivity to γ. There are also favoured decays, where the $b \to c\bar{u}s$ transition is followed by a favoured D meson decay. These have little interference and weak sensitivity to γ, but provide appropriate normalisation for the suppressed decays.

A search for $b \to u\bar{c}s$ amplitudes contributing to $B^- \to DK^-$ decays was first performed with the $D \to K\pi\pi^0$ mode by the BaBar collaboration [8]. Later, evidence of the suppressed $B^- \to [\pi^-K^+\pi^0]_DK^-$ decay was reported by the BELLE collaboration [9] and LHCb [10]. This work supersedes Ref. [10] with a fourfold increase in data.

2 External inputs and formalism

Three-body GLW modes, like those considered in this paper: $D \to \pi^-\pi^+\pi^0$ and $D \to K^-K^+\pi^0$, are an admixture of *CP*-even and *CP*-odd eigenstates. *CP*-even and *CP*-odd states exhibit opposite *CP* asymmetry so integrating over the three-body phase space dilutes sensitivity to γ. This dilution is parameterised by *CP*-even fractions: $F_+^{\pi\pi\pi^0}$ and $F_+^{KK\pi^0}$. A *CP*-even fraction of zero implies a pure *CP*-odd state, 0.5 means an equal amount of *CP*-even and *CP*-odd states contributing to the multibody decay. The *CP*-even fractions relevant to this analysis have been measured with quantum-correlated $D\overline{D}$ pairs

[1] The inclusion of charge-conjugate modes is implied everywhere except when discussing asymmetries.

produced at the $\psi(3770)$ resonance: $F_+^{\pi\pi\pi^0} = 0.973 \pm 0.017$ and $F_+^{KK\pi^0} = 0.732 \pm 0.055$ are measured in Refs. [11, 12].

In the case of the non-charge-conjugate ADS mode, both the Cabibbo-suppressed $\overline{D}^0 \to K^-\pi^+\pi^0$ and favoured $D^0 \to K^-\pi^+\pi^0$ amplitudes contribute. The ratio of their magnitudes, $r_D = 0.0441 \pm 0.0011$ [13] is similar to r_B, hence the possibility of large *CP* asymmetries. In the ADS case, the dilution is parameterised by a coherence factor, $\kappa_D = 0.79 \pm 0.04$. This number and the average strong phase difference between $\overline{D}^0 \to K^-\pi^+\pi^0$ and $D^0 \to K^-\pi^+\pi^0$ amplitudes, $\delta_D = (196 \pm 11)^\circ$, are reported in Ref. [13]. The relatively high value of κ_D means that integrating over the whole three-body D decay phase space retains sensitivity to γ.

Incorporating the effect of D meson mixing up to first order in x and y [14], the partial rate expression for the ADS modes is

$$\begin{aligned}\Gamma(B^\mp \to [\pi^\mp K^\pm \pi^0]_D h^\mp) \;\propto\; & r_D^2 + r_B^2 + 2 r_D r_B \kappa_D \cos(\delta_B + \delta_D \mp \gamma) \\ & - \alpha y (1 + r_B^2) r_D \kappa_D \cos\delta_D - \alpha y (1 + r_D^2) r_B \cos(\delta_B \mp \gamma) \\ & + \alpha x (1 - r_B^2) r_D \kappa_D \sin\delta_D - \alpha x (1 - r_D^2) r_B \sin(\delta_B \mp \gamma),\end{aligned} \tag{1}$$

where $x = (0.409^{+0.048}_{-0.049})\%$ and $y = (0.615^{+0.056}_{-0.055})\%$ are the charm mixing parameters [2] and α is an analysis-specific coefficient that quantifies the decay-time acceptance of the candidate D mesons. This coefficient is determined from simulation, to be $\alpha = 1.0$ with negligible uncertainty. The same rate expression is used for GLW mode f, where $r_D \equiv 1$, $\delta_D \equiv 0$ and $\kappa_D = 2F_+^f - 1$. For completeness, the equivalent rate for the favoured mode is

$$\begin{aligned}\Gamma(B^\mp \to [K^\mp \pi^\pm \pi^0]_D h^\mp) \;\propto\; & 1 + r_D^2 r_B^2 + 2 r_D r_B \kappa_D \cos(\delta_B - \delta_D \mp \gamma) \\ & - \alpha y (1 + r_B^2) r_D \kappa_D \cos\delta_D - \alpha y (1 + r_D^2) r_B \cos(\delta_B \mp \gamma) \\ & - \alpha x (1 - r_B^2) r_D \kappa_D \sin\delta_D + \alpha x (1 - r_D^2) r_B \sin(\delta_B \mp \gamma).\end{aligned} \tag{2}$$

The *CP* observables reported in this paper are all experimentally-robust ratios of decay rates. From the ADS modes, two ratios of suppressed to favoured decay rates are measured independently for B^- and B^+ decays,

$$R_K^\mp \equiv \frac{\Gamma(B^\mp \to [\pi^\mp K^\pm \pi^0]_D K^\mp)}{\Gamma(B^\mp \to [K^\mp \pi^\pm \pi^0]_D K^\mp)}, \tag{3}$$

$$R_\pi^\mp \equiv \frac{\Gamma(B^\mp \to [\pi^\mp K^\pm \pi^0]_D \pi^\mp)}{\Gamma(B^\mp \to [K^\mp \pi^\pm \pi^0]_D \pi^\mp)}. \tag{4}$$

For the GLW modes two *CP* asymmetries are measured,

$$A_K^{hh\pi^0} = \frac{\Gamma(B^- \to [hh\pi^0]_D K^-) - \Gamma(B^+ \to [hh\pi^0]_D K^+)}{\Gamma(B^- \to [hh\pi^0]_D K^-) + \Gamma(B^+ \to [hh\pi^0]_D K^+)}, \tag{5}$$

$$A_\pi^{hh\pi^0} = \frac{\Gamma(B^- \to [hh\pi^0]_D \pi^-) - \Gamma(B^+ \to [hh\pi^0]_D \pi^+)}{\Gamma(B^- \to [hh\pi^0]_D \pi^-) + \Gamma(B^+ \to [hh\pi^0]_D \pi^+)} \tag{6}$$

where h is either a kaon or a pion. Two double ratios are constructed,

$$R^{KK\pi^0} = R_{K/\pi}^{KK\pi^0} / R_{K/\pi}^{K\pi\pi^0}, \qquad R^{\pi\pi\pi^0} = R_{K/\pi}^{\pi\pi\pi^0} / R_{K/\pi}^{K\pi\pi^0}, \tag{7}$$

where

$$R_{K/\pi}^{hh\pi^0} = \frac{\Gamma(B^- \to [hh\pi^0]_D K^-) + \Gamma(B^+ \to [hh\pi^0]_D K^+)}{\Gamma(B^- \to [hh\pi^0]_D \pi^-) + \Gamma(B^+ \to [hh\pi^0]_D \pi^+)} \tag{8}$$

is the ratio of the summed-over-charge partial widths for the $B^- \to DK^-$ decays over the $B^- \to D\pi^-$ decays for a given D meson decay mode. Last, the *CP* asymmetry in the favoured mode is also included, though the expectation from Eq. 2 is that the *CP* asymmetry is only $\mathcal{O}(1\%)$,

$$A_K^{K\pi\pi^0} = \frac{\Gamma(B^- \to [K^-\pi^+\pi^0]_D K^-) - \Gamma(B^+ \to [K^+\pi^-\pi^0]_D K^+)}{\Gamma(B^- \to [K^-\pi^+\pi^0]_D K^-) + \Gamma(B^+ \to [K^+\pi^-\pi^0]_D K^+)}. \tag{9}$$

To summarise, 11 observables are reported: four ADS ratios $R_h^{\mp}$, four GLW asymmetries $A_h^{hh\pi^0}$, two double ratios $R^{hh\pi^0}$ and the favoured-mode asymmetry, $A_K^{K\pi\pi^0}$.

3 The LHCb detector

The analysis uses data collected by the LHCb experiment in proton-proton (pp) collisions at $\sqrt{s} = 7\,\text{TeV}$, $8\,\text{TeV}$, and $13\,\text{TeV}$, corresponding to integrated luminosities of $1\,\text{fb}^{-1}$, $2\,\text{fb}^{-1}$, and $6\,\text{fb}^{-1}$ respectively.

The LHCb detector [15, 16] is a single-arm forward spectrometer covering the pseudorapidity range $2 < \eta < 5$, designed for the study of particles containing b or c quarks. The detector includes a high-precision tracking system consisting of a silicon-strip vertex detector surrounding the pp interaction region, a large-area silicon-strip detector located upstream of a dipole magnet with a bending power of about $4\,\text{Tm}$, and three stations of silicon-strip detectors and straw drift tubes placed downstream of the magnet. The tracking system provides a measurement of the momentum, p, of charged particles with a relative uncertainty that varies from 0.5% at low momentum to 1.0% at $200\,\text{GeV}/c$. The minimum distance of a track to a primary pp collision vertex (PV), the impact parameter (IP), is measured with a resolution of $(15 + 29/p_\text{T})\,\mu\text{m}$, where p_T is the component of the momentum transverse to the beam, in GeV/c. Different types of charged hadrons are distinguished using information from two ring-imaging Cherenkov (RICH) detectors. Photons, electrons and hadrons are identified by a calorimeter system consisting of scintillating-pad and preshower detectors, an electromagnetic and a hadronic calorimeter. For the photons used to reconstruct π^0 candidates in this analysis, the relative uncertainty on their energy measurement is $\sim 6.5\%$. Muons are identified by a system composed of alternating layers of iron and multiwire proportional chambers. The online event selection is performed by a trigger, which consists of a hardware stage, based on information from the calorimeter and muon systems, followed by a software stage, which applies a full event reconstruction.

Simulated events of each class of signal decay are used in the analysis. In the simulation pp collisions are generated using Pythia [17] with a specific LHCb configuration. Decays of hadrons are described by EvtGen [18], in which final-state radiation is generated using Photos [19]. The interaction of the generated particles with the detector, and its response, are implemented using the Geant4 toolkit [20] as described in Ref. [21].

4 Event selection

The study is performed with $B^- \to Dh^-$ candidates, where the neutral D candidate is reconstructed in a three-body final state composed of two charged tracks and a π^0

candidate. These charged tracks and the companion charged track used to reconstruct the B^- candidate are identified as either a kaon or pion. The π^0 candidate is reconstructed from two photons, as recorded by the electromagnetic calorimeter.

The mass of the reconstructed D candidate is required to be within $\pm 50\,\mathrm{MeV}/c^2$ of the known D^0 mass [22]. The mass of the π^0 candidate must be within $\pm 20\,\mathrm{MeV}/c^2$ of the known π^0 mass [22]. Both of these mass windows correspond to approximately twice the mass resolution of the detector. The $B^- \to Dh^-$ candidates are required to have a mass in the range $5000 - 5900\,\mathrm{MeV}/c^2$. The π^0 candidate must also have p above $1\,\mathrm{GeV}/c$ and p_T greater than $0.5\,\mathrm{GeV}/c$. The companion particle is required to satisfy $0.5 < p_\mathrm{T} < 10\,\mathrm{GeV}/c$ and $5 < p < 100\,\mathrm{GeV}/c$, while the charged decay products from the D meson must have $p_\mathrm{T} > 0.25\,\mathrm{GeV}/c$. The mass resolution of the B^- candidate is improved with a fit [23] that constrains the D candidate to its nominal mass and requires the candidate to point back to the primary pp interaction vertex. Events are required to have been selected by the trigger in one of two ways: by tracks from the B^- candidate activating the hadronic calorimeter; or by activity in the rest of the event, independent of the B^- candidate.

Further background suppression is achieved with a boosted decision tree (BDT) [24,25] classifier. The BDT classifier is trained using a simulated $B^- \to Dh^-$ signal sample and a sample of combinatorial background taken from data where the B candidate mass is above $5500\,\mathrm{MeV}/c^2$. The background sample is subdivided in two parallel procedures to ensure the classifier is not applied to events against which it was trained. The properties used as input to the BDT training are: the p and p_T of the D candidate, the π^0, and the companion particle; the χ^2 per degree of freedom for the B^- candidate vertex fit; the χ^2_IP of the B^- and D candidates, where χ^2_IP is defined as the difference between the χ^2 of the PV reconstructed with and without the particle of interest; the flight distance from the PV for both the B^- and D candidates; the angle between a line connecting the particle's decay vertex from the PV and the particle's momentum vector, for both the B^- and D candidates; the particle identification (PID) confidence level of both photons constituting the π^0 candidate; and the sum of charged-track transverse momenta within a cone surrounding the B^- candidate direction.

The selection requirement on the BDT output optimises the metric $s/\sqrt{s+b}$, where s is the expected signal yield in the suppressed $B^- \to DK^-$ ADS mode and b is the combinatorial background level as taken from a fit to the favoured mode. This assumes that the suppressed and favoured modes suffer a comparable level of random D and h^- combinations. The expected signal yield is calculated as the yield of the favoured $B^- \to D\pi^-$ mode scaled by the ratio of expected branching fractions while taking into account the relative difference in companion particle PID efficiency. Since the BDT discriminant includes no variables related to the D decay products the same BDT requirement is used for the selection of GLW and ADS modes.

PID from the RICH detectors is essential to distinguish $B^- \to DK^-$ decays among the more abundant $B^- \to D\pi^-$ candidates. The PID algorithm considers the likelihood of the pattern of RICH photons under K and π mass hypotheses, $\mathcal{L}_{K,\pi}$. The companion particle in $B^- \to DK^-$ candidates is required to pass a tight selection requiring a high value of $(\ln\mathcal{L}_K - \ln\mathcal{L}_\pi)$. Candidates failing this selection are treated as $B^- \to D\pi^-$ candidates in the mass fit. Looser but mutually exclusive selection requirements are placed on the kaon and pion from the D meson decay.

Additional restrictions are imposed after the application of the BDT classifier and the PID requirements in order to remove specific sources of background. Contributions

from genuine B^- meson decays that do not include a D meson (charmless background) are suppressed by a requirement on the flight distance significance, FD_D, defined as the distance between the D and B^- meson candidate vertices divided by the uncertainty on this measurement. A requirement of $\mathrm{FD}_D > 2$ is applied. The relevant branching fractions of $B^- \to hhh\pi^0$ decays are currently unmeasured and their contribution is estimated by measuring the number of B^- candidates in the D-mass sideband regions (defined as $1615 - 1715\,\mathrm{MeV}/c^2$ and $2015 - 2115\,\mathrm{MeV}/c^2$) after the FD_D selection has been applied. Charmless background remains in the $B^- \to [\pi^-\pi^+\pi^0]_D K^-$ sidebands after the FD_D requirement. The average charmless yield from the lower and upper sidebands is measured and fixed as the charmless background in the signal region fit of this mode.

The suppressed ADS decays, $B^- \to [\pi^- K^+\pi^0]_D h^-$, are subject to potential contamination from the GLW modes where one of the charged pions (kaons) from the D candidate is misidentified as a kaon (pion). Simulation demonstrates that such contamination is minimal because a single misidentification among the D decay products moves the D candidate invariant mass out of the D-mass window. The suppressed decays suffer crossfeed in the D-mass window when a true $K^-\pi^+$ pair from favoured $B^- \to [K^-\pi^+\pi^0]_D h^-$ decays is misidentified as a $\pi^- K^+$ candidate by the PID system. This background is reduced by vetoing any suppressed mode candidate whose reconstructed D mass, under the exchange of mass hypotheses between the kaon and charged pion, lies within $\pm 30\,\mathrm{MeV}/c^2$ of the nominal D meson mass. The residual contamination is estimated by studying the crossfeed remaining in the D-mass sidebands, and knowledge of the PID efficiency. The residual crossfeed, expressed as a fraction of the favoured decay yield, is $(0.85 \pm 0.04) \times 10^{-4}$, which is about 3% of the size of the $R_\pi^\mp$ observable. Finally, after all selection, 4% of events contain more than one B^- candidate. In these cases a single candidate is selected at random.

5 Mass fit

The observables defined in Sec. 2 are determined with a binned maximum-likelihood fit to the mass distribution of the selected B^- candidates. A total of sixteen subsamples are fitted simultaneously: the favoured modes; the suppressed ADS modes; and the two GLW modes, each separated according to the charge of the B^- candidate, and by the companion track PID. $B^- \to DK^-$ candidates are defined as those that pass a PID requirement intended to remove $> 99\%$ of $B^- \to D\pi^-$ decays; $B^- \to D\pi^-$ candidates are defined as those failing this requirement. The mass spectra are presented in Figs. 1 to 4. The total probability density function (PDF) used in the fit is built from five main components, described below, which represent the different categories of signal and background.

The mass (m) distribution of $B^- \to D\pi^-$ signal candidates is modelled through the use of a modified Gaussian function

$$f(m;\mu,\sigma,\alpha_L,\alpha_R,\beta) = \exp\left(\frac{-(m-\mu)^2(1+\beta(m-\mu)^2)}{2\sigma^2+\alpha(m-\mu)^2}\right) \tag{10}$$

where, $\alpha = \alpha_L$ for $m < \mu$ and $\alpha = \alpha_R$ otherwise. This expression describes an asymmetric peak of mean μ and width σ. The tails of the distribution are parameterised on the left (right) side of the peak by $\alpha_{L(R)}$; the term involving the parameter β ensures finite normalisation. All of these parameters vary freely in the fit. The $B^- \to DK^-$ signal is

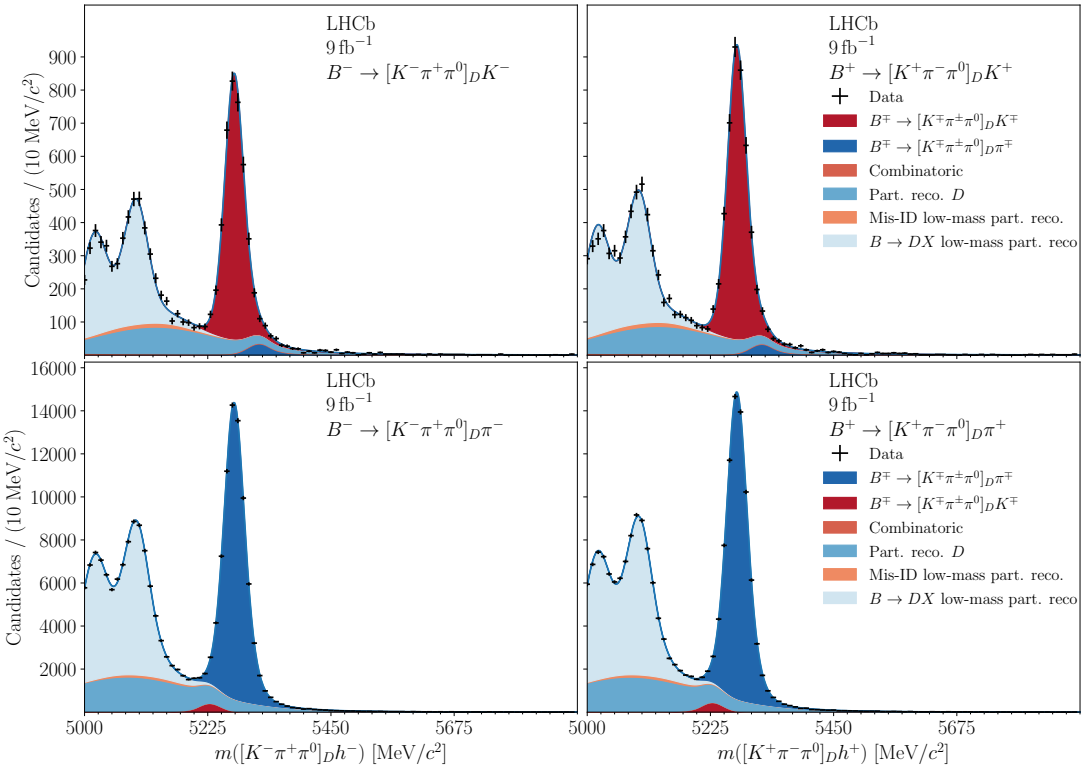

Figure 1: Mass distributions of $B^\mp \to [K^\mp\pi^\pm\pi^0]_D K^\mp$ (top) and $B^\mp \to [K^\mp\pi^\pm\pi^0]_D \pi^\mp$ (bottom) candidates, separated by charge.

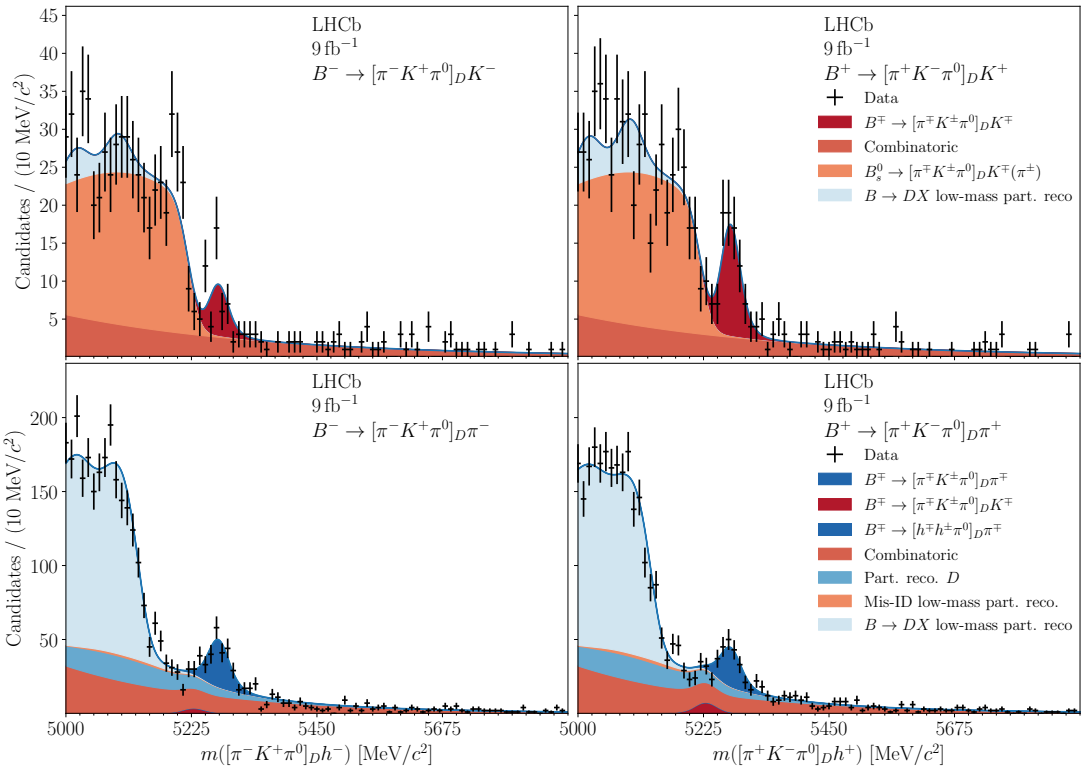

Figure 2: Mass distributions of $B^\mp \to [\pi^\mp K^\pm\pi^0]_D K^\mp$ (top) and $B^\mp \to [\pi^\mp K^\pm\pi^0]_D \pi^\mp$ (bottom) candidates, separated by charge.

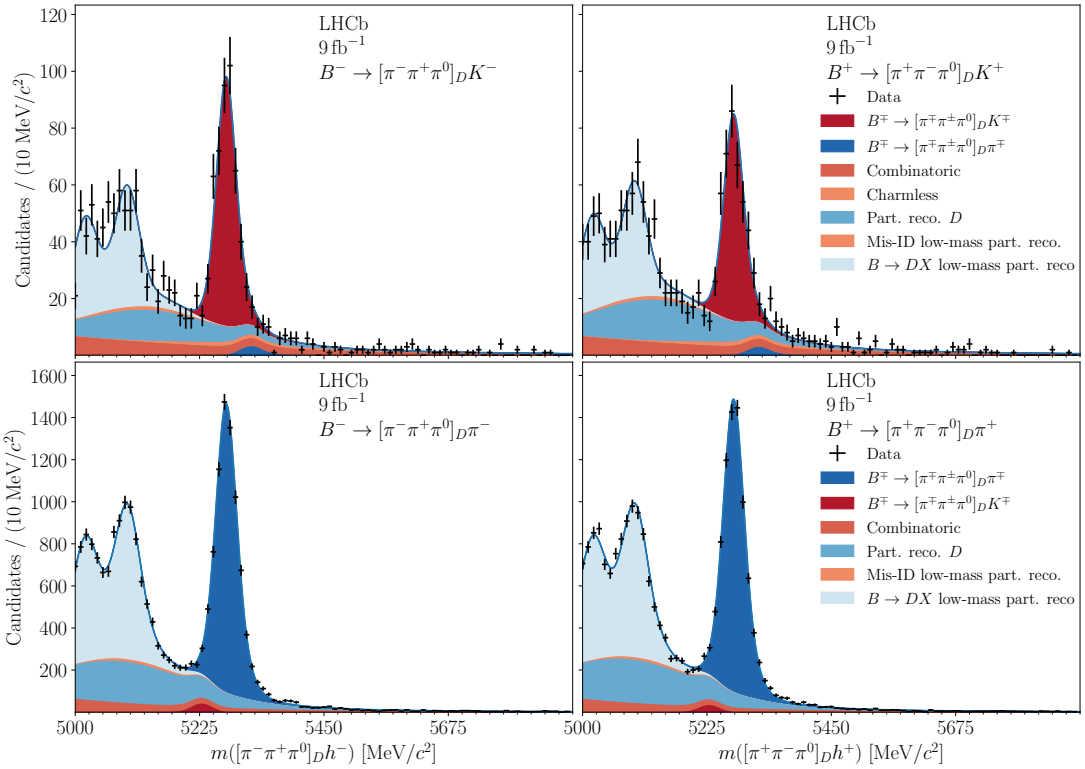

Figure 3: Mass distributions of $B^\mp \to [\pi^\pm\pi^\mp\pi^0]_D K^\mp$ (top) and $B^\mp \to [\pi^\pm\pi^\mp\pi^0]_D \pi^\mp$ (bottom) candidates, separated by charge.

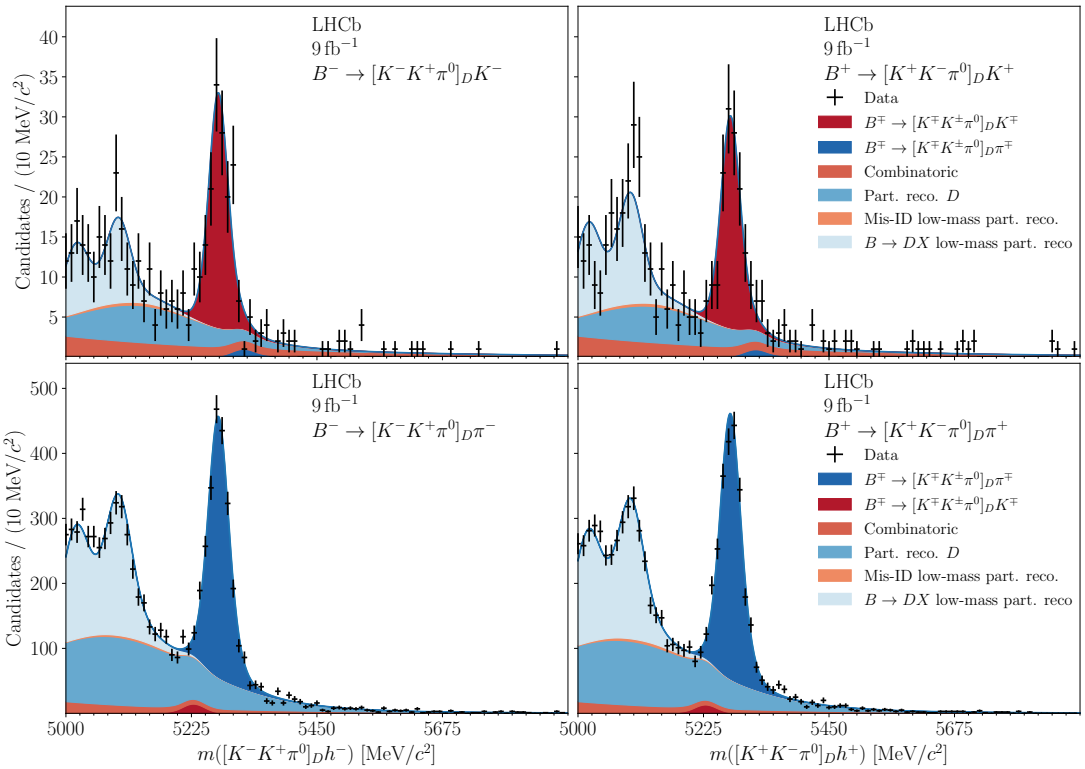

Figure 4: Mass distributions of $B^\mp \to [K^\pm K^\mp\pi^0]_D K^\mp$ (top) and $B^\mp \to [K^\pm K^\mp\pi^0]_D \pi^\mp$ (bottom) candidates, separated by charge.

modelled using the same modified Gaussian function of Eq. 10. All of the parameters are identical to those of the $B^- \to D\pi^-$ modes except for the width, which is related to that of the $B^- \to D\pi^-$ by a ratio parameter that is allowed to vary in the fit. The $B^- \to [KK\pi^0]_D h^-$ ($B^- \to [\pi\pi\pi^0]_D h^-$) signal peaks are slightly narrower (wider) than the $B^- \to [K\pi\pi^0]_D h^-$ peaks; fixed factors that modify the peak width in these modes are taken from simulation.

$B^- \to D\pi^-$ decays misidentified as $B^- \to DK^-$ candidates are modelled by the sum of two modified Gaussian functions that share a mean and width but have two sets of tail parameters. $B^- \to DK^-$ decays misidentified as $B^- \to D\pi^-$ candidates are described using a single modified Gaussian function. Misidentified events form a small background so all their parameters are fixed to the values derived from simulation.

Partially reconstructed b-hadron decays populate the mass region below the B^- mass though their tails can enters the signal region. Of particular concern are $B^-(B^0)$ decays involving a neutral (charged) D^* meson decaying to a D^0 candidate plus an unreconstructed neutral (charged) pion. Similarly, $B^- \to D^{*0}h^-$, $D^{*0} \to D\gamma$ decays mimic the signal because the γ is not reconstructed. There are also contributions from $B^-(B^0)$ decays to a D and a neutral (charged) ρ or K^* vector meson decaying to an $h^+\pi^-(h^+\pi^0)$ state from which the $\pi^-(\pi^0)$ is missed in reconstruction. These partially reconstructed decays are described by parabolic functions convolved with a double Gaussian to account for detector resolution [26]. The yields of these background components vary independently in the fit, with no assumption of CP symmetry. Additionally, partially reconstructed $B_s^0 \to \overline{D}^0 K^-\pi^+$ decays are an important background for the ADS $B^- \to DK^-$ signal. PDFs for this background are determined from simulation weighted with an amplitude model [27] and fixed in the fit. The B_s^0 yields are allowed to vary freely, but CP symmetry is assumed because only the $b \to c\overline{u}s$ transition amplitude contributes significantly.

Wrongly reconstructed D meson decays are a significant source of background under the signal peaks. These are primarily decays where the π^0 candidate is not a decay product of the D meson, but is wrongly assigned as such. These contributions are modelled using the modified Gaussian function of Eq. 10 with a large right-hand tail. This PDF is defined from an ancillary fit to the B mass distribution in the D-mass sideband. The tail and mean parameters are fixed by this procedure but the width is allowed to vary freely in the main fit to account for kinematic differences between the sideband and the signal regions. The fixed parameters are varied as a source of systematic uncertainty.

The combinatorial background of unassociated D and h^- candidates is modelled using an exponential function, with a common slope for all $B^- \to DK^-$ modes and a second for all $B^- \to D\pi^-$ modes. The favoured and suppressed modes share the same combinatorial background yield. The GLW modes have independently floating combinatorial yields and CP symmetry is imposed in all cases.

The observables defined in Section 1 vary freely in the fit as well as the total $B^- \to D\pi^-$ yields. The individual signal yields are derived from these values and are presented in Table 1. The correlation of the statistical uncertainties for the observables are summarised in Table 3 of Appendix A.

Table 1: Signal yields for each decay mode. The uncertainties quoted are statistical only.

Mode	Yield
$B^\pm \to [K^\pm K^\mp \pi^0]_D \pi^\pm$	4026 ± 77
$B^\pm \to [\pi^\pm \pi^\mp \pi^0]_D \pi^\pm$	14180 ± 140
$B^\pm \to [K^\pm \pi^\mp \pi^0]_D \pi^\pm$	140696 ± 589
$B^\pm \to [\pi^\pm K^\mp \pi^0]_D \pi^\pm$	293 ± 27
$B^\pm \to [K^\pm K^\mp \pi^0]_D K^\pm$	401 ± 29
$B^\pm \to [\pi^\pm \pi^\mp \pi^0]_D K^\pm$	1189 ± 51
$B^\pm \to [K^\pm \pi^\mp \pi^0]_D K^\pm$	12265 ± 158
$B^\pm \to [\pi^\pm K^\mp \pi^0]_D K^\pm$	155 ± 19

6 Systematic uncertainties

Where fixed parameters are necessary for fit stability, they are varied systematically to assess their contribution to the overall uncertainty. The dominant fixed-parameter effect comes from the wrongly-reconstructed D-meson PDF, where the systematic variation is defined by the covariance matrix of the ancillary fits to the sideband distributions.

The efficiency and uncertainty of the PID requirements on the companion track are determined from a sample of more than 100 million $D^{*\pm}$ decays reconstructed as $D^{*\pm} \to D\pi^\pm$ with $D \to K^\mp \pi^\pm$. This reconstruction is performed entirely using kinematic variables and provides a high-purity calibration sample of $K^\pm$ and $\pi^\pm$ tracks. The PID efficiency varies as a function of track momentum, pseudorapidity, and detector occupancy. The average PID efficiency of the signal is determined by reweighting the calibration spectra in these variables to those of the candidates in the favoured mode sample. This average PID efficiency is evaluated to be 64.2% and 99.7% for kaons and pions, respectively. Systematic uncertainties of 0.7% and 0.1% for companion kaons and companion pions are attributed to the reweighting procedure in the efficiency determination. These uncertainties are estimated by varying the binning scheme used in the calibration procedure.

Due to their differing interaction lengths, a small negative asymmetry is expected in the detection efficiency of K^- and K^+ mesons. The difference between the kaon and pion detection asymmetries is expected to be $(-0.869 \pm 0.165)\%$ and a raw asymmetry of $(-0.17 \pm 0.10)\%$ is used for pions. These numbers are taken from a dedicated study [28] and also account for any physical asymmetry between the left and right sides of the LHCb detector. There is no systematic uncertainty from the difference in B^- and B^+ production cross sections because this effect is absorbed into a global asymmetry parameter, dominated by the favoured $B^- \to D\pi^-$ decay, that is free to vary in the fit. All quoted CP asymmetries are automatically corrected for this value.

The $R^{hh\pi^0}_{K/\pi}$ observables must be corrected for the ratio of efficiencies of $B^- \to DK^-$ decays relative to $B^- \to D\pi^-$ decays. These ratios quantify the efficiency differences due to the trigger, reconstruction and selection. They are measured in simulation to be $(92.6 \pm 2.3)\%$ for the $B^- \to [K^-\pi^+\pi^0]_D h^-$ and $B^- \to [\pi^- K^+ \pi^0]_D h^-$ modes, $(98.7 \pm 2.8)\%$ for the $B^- \to [\pi^-\pi^+\pi^0]_D h^-$ modes, and $(103.7 \pm 2.9)\%$ for the $B^- \to [K^- K^+ \pi^0]_D h^-$ modes. The uncertainties listed are based on the finite size of the simulated samples and are large enough to account for any inaccuracies in the simulation.

In order to estimate the systematic uncertainties from the sources described in this

Table 2: Systematic uncertainties on the observables, multiplied by 10^4. PID refers to the fixed PID efficiencies of the companion tracks. PDFs refers to the uncertainties in fixing parameters in the fit PDF. Sim refers to the use of simulation to calculate relative efficiencies between the $B^- \to DK^-$ and $B^- \to D\pi^-$ modes. $A_{\rm instr}$ refers to the interaction and detection asymmetries. D decay refers to the effect of assuming that the distribution of candidates in the D meson decay phase-space is not sculpted by the selection. The Total column corresponds to the quadrature sum over the five categories.

	PID	PDFs	Sim	$A_{\rm instr}$	D decay	Total
$A_K^{KK\pi^0}$	6.9	11.7	8.2	0.1	21.4	26.6
$A_K^{K\pi\pi^0}$	7.2	1.2	2.3	16.7	1.7	18.4
$A_K^{\pi\pi\pi^0}$	8.2	12.2	16.2	0.1	22.2	31.1
$A_\pi^{KK\pi^0}$	1.6	1.4	1.0	16.7	0.0	16.9
$A_\pi^{\pi\pi\pi^0}$	1.5	0.7	1.3	16.7	0.0	16.8
$R^{KK\pi^0}$	24.5	28.8	31.9	0.1	5.3	49.8
$R^{\pi\pi\pi^0}$	15.8	26.7	24.6	0.1	5.3	40.0
R_K^-	0.7	1.3	0.8	0.1	3.4	3.8
R_π^-	0.0	0.2	0.2	0.1	0.3	0.4
R_K^+	0.8	1.1	1.3	0.3	2.3	3.0
R_π^+	0.0	0.2	0.2	0.1	0.4	0.5

section, the fit is performed many times, varying each source by its assigned uncertainty, under the assumption that a Gaussian distribution is appropriate. When sources of systematic uncertainty are correlated, *e.g.* the fixed parameters of a PDF, the variations are drawn from a multidimensional Gaussian distribution according to the associated covariance matrix. The spread of the fit result for each *CP* observables is taken as the systematic uncertainty for that quantity. These uncertainties are summarised in Table 2. The correlations of the systematic uncertainties are recorded in Table 4 of Appendix A.

The values for the coherence factor, average strong-phase differences and *CP*-even fraction are reported in Refs [11–13, 29–31] for a uniform acceptance across the three-body phase space of the D meson decay, which is not the case in this analysis. To assess the impact of an imperfect acceptance, studies are performed with amplitude models for each D mode and an acceptance function derived from simulation. The study shows that this is the dominant systematic uncertainty for $A_K^{KK\pi^0}$, $A_K^{\pi\pi\pi^0}$, $R_K^\pm$, and $R_\pi^\pm$ with an effect in the range $(5 \sim 26)\%$ of the magnitude of the associated statistical uncertainty.

7 Results

The final results, as determined by the fit and systematic uncertainty assessment, are

$$
\begin{array}{rcrcrcl}
R^{KK\pi^0} & = & 1.021 & \pm & 0.079 & \pm & 0.005 \\
R^{\pi\pi\pi^0} & = & 0.902 & \pm & 0.041 & \pm & 0.004 \\
A_K^{K\pi\pi^0} & = & -0.024 & \pm & 0.013 & \pm & 0.002 \\
A_K^{KK\pi^0} & = & 0.067 & \pm & 0.073 & \pm & 0.003 \\
A_K^{\pi\pi\pi^0} & = & 0.109 & \pm & 0.043 & \pm & 0.003 \\
A_\pi^{KK\pi^0} & = & -0.001 & \pm & 0.019 & \pm & 0.002 \\
A_\pi^{\pi\pi\pi^0} & = & 0.001 & \pm & 0.010 & \pm & 0.002 \\
R_K^+ & = & 0.0179 & \pm & 0.0024 & \pm & 0.0003 \\
R_K^- & = & 0.0085 & \pm & 0.0020 & \pm & 0.0004 \\
R_\pi^+ & = & 0.00188 & \pm & 0.00027 & \pm & 0.00005 \\
R_\pi^- & = & 0.00227 & \pm & 0.00028 & \pm & 0.00004,
\end{array}
$$

where the statistical uncertainties are listed first and the systematic uncertainties second. All results are compatible with, but better than, previous measurements. The four $R_h^\pm$ observables can be used to calculate

$$
\begin{array}{rcrcrcl}
R_{\mathrm{ADS}(K)} & = & 0.0127 & \pm & 0.0016 & \pm & 0.0002 \\
A_{\mathrm{ADS}(K)} & = & -0.38 & \pm & 0.12 & \pm & 0.02 \\
R_{\mathrm{ADS}(\pi)} & = & 0.00207 & \pm & 0.00020 & \pm & 0.00003 \\
A_{\mathrm{ADS}(\pi)} & = & 0.069 & \pm & 0.094 & \pm & 0.016,
\end{array}
$$

where

$$
R_{\mathrm{ADS}(h)} = \frac{\Gamma(B^- \to [\pi^- K^+ \pi^0]_D h^-) + \Gamma(B^+ \to [\pi^+ K^- \pi^0]_D h^+)}{\Gamma(B^- \to [K^- \pi^+ \pi^0]_D h^-) + \Gamma(B^+ \to [K^+ \pi^- \pi^0]_D h^+)} \tag{11}
$$

and

$$
A_{\mathrm{ADS}(h)} = \frac{\Gamma(B^- \to [\pi^- K^+ \pi^0]_D h^-) - \Gamma(B^+ \to [\pi^+ K^- \pi^0]_D h^+)}{\Gamma(B^- \to [\pi^- K^+ \pi^0]_D h^-) + \Gamma(B^+ \to [\pi^+ K^- \pi^0]_D h^+)}. \tag{12}
$$

A likelihood-ratio test is used to assess the significance of the previously-unobserved $B^- \to DK^-$ ADS signal [32]. This is performed by calculating the quantity $\sqrt{-2\ln(\mathcal{L}_b/\mathcal{L}_{s+b})}$ where $\mathcal{L}_b$ and $\mathcal{L}_{s+b}$ are the maximum-likelihood values of the background-only and signal-plus-background hypotheses, respectively. Including systematic uncertainties, a significance of 7.8 standard deviations (σ) is found for the decay $B^- \to [\pi^- K^+ \pi^0]_D K^-$.

8 Interpretation and conclusions

The results are interpreted in terms of the fundamental parameters: γ; r_B and δ_B using Eqs. 1-2 and inputs from Refs [11–13, 29–31]. Confidence intervals are evaluated using the profile likelihood method. For this, the χ^2 function is evaluated at each point in parameter space to determine a $\Delta\chi^2$ with respect to the best-fit point. Assuming purely Gaussian behaviour, the plotted p-value, $p \equiv 1 - \mathrm{CL}$, is given by the probability that $\Delta\chi^2$ is distributed according to a χ^2 distribution with one degree of freedom. Due to trigonometric ambiguities present in Eq. 1, there are up to four solutions in the range $0 < \gamma < 180^\circ$. The global minimum χ^2 is found at $\gamma = (145^{+\,9}_{-39})^\circ$ but a second solution, close to the established value [33], is also found and quoted below. Two-dimensional confidence regions are shown in Fig. 5 focusing on the second solution. The values of γ and the $B^- \to DK^-$ hadronic parameters, δ_B and r_B, found from this analysis are

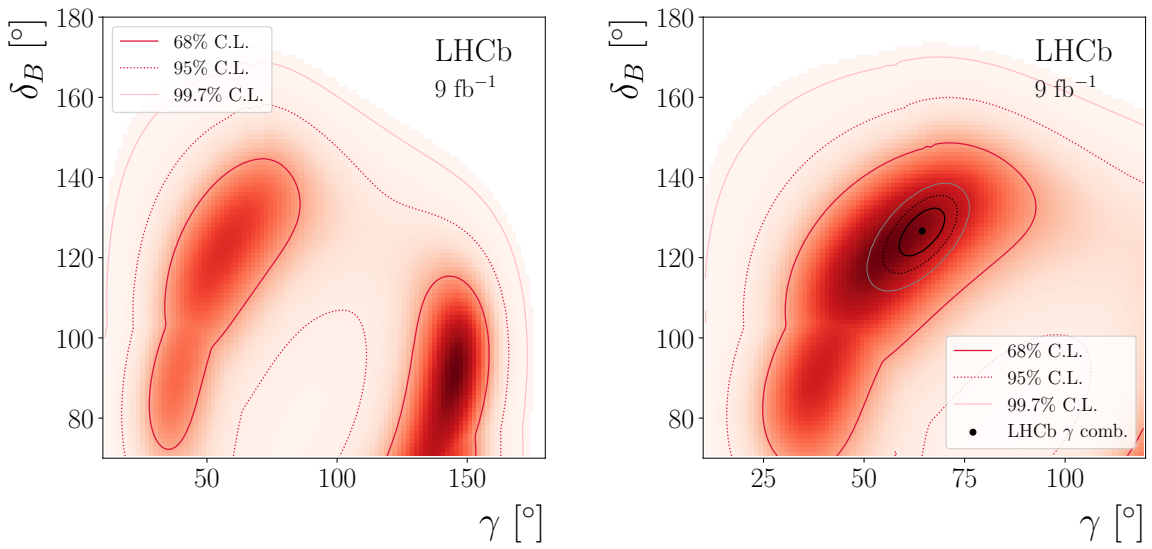

Figure 5: Confidence regions of the strong phase, δ_B versus the unitarity triangle angle, γ shows (left) two solutions, one of which is shown (right) to be consistent with the 2021 γ combination result [33] whose confidence intervals are superimposed.

$$\begin{aligned} \gamma &= (56^{+24}_{-19})^\circ, \\ \delta_B &= (122^{+19}_{-23})^\circ, \\ r_B &= (9.3^{+1.0}_{-0.9}) \times 10^{-2}, \end{aligned}$$

with only weak limits found for the $B^- \to D\pi^-$ hadronic parameters. The corresponding confidence regions for the 2021 LHCb γ combination [33] are shown for comparison. This new result is consistent with the combination.

In conclusion, using a dataset of pp collisions corresponding to an integrated luminosity of 9 fb^{-1}, $B^- \to DK^-$ and $B^- \to D\pi^-$ decays are studied where the charm meson is reconstructed in the $K^-\pi^+\pi^0$, $\pi^+\pi^-\pi^0$, $K^+K^-\pi^0$ or $\pi^-K^+\pi^0$ final states. Eleven CP observables are measured with world-best precision. The suppressed $B^- \to [\pi^-K^+\pi^0]_D K^-$ mode is observed for the first time, with a significance of $7.8\,\sigma$ and evidence for a large CP asymmetry in this mode is reported. The suppressed-to-favoured ratios, $R_{\mathrm{ADS}(K)}$ and $R_{\mathrm{ADS}(\pi)}$ are 42 and seven times larger than the doubly-Cabibbo-suppressed $\mathcal{B}(D^0 \to \pi^-K^+\pi^0) = (3.05 \pm 0.15) \times 10^{-4}$ [22]. In addition to the CP asymmetry, this underlines the presence and importance of the $b \to u$ transition amplitude contributing to $B^\pm \to [h^\pm h'^\mp\pi^0]_D h^\pm$ decays. In combination with similar $B \to DX$ measurements, these results will contribute to a precise determination of the CKM Unitary Triangle angle γ.

Acknowledgements

We express our gratitude to our colleagues in the CERN accelerator departments for the excellent performance of the LHC. We thank the technical and administrative staff at the LHCb institutes. We acknowledge support from CERN and from the national agencies: CAPES, CNPq, FAPERJ and FINEP (Brazil); MOST and NSFC (China); CNRS/IN2P3 (France); BMBF, DFG and MPG (Germany); INFN (Italy); NWO (Netherlands); MNiSW

and NCN (Poland); MEN/IFA (Romania); MSHE (Russia); MICINN (Spain); SNSF and SER (Switzerland); NASU (Ukraine); STFC (United Kingdom); DOE NP and NSF (USA). We acknowledge the computing resources that are provided by CERN, IN2P3 (France), KIT and DESY (Germany), INFN (Italy), SURF (Netherlands), PIC (Spain), GridPP (United Kingdom), RRCKI and Yandex LLC (Russia), CSCS (Switzerland), IFIN-HH (Romania), CBPF (Brazil), PL-GRID (Poland) and NERSC (USA). We are indebted to the communities behind the multiple open-source software packages on which we depend. Individual groups or members have received support from ARC and ARDC (Australia); AvH Foundation (Germany); EPLANET, Marie Skłodowska-Curie Actions and ERC (European Union); A*MIDEX, ANR, IPhU and Labex P2IO, and Région Auvergne-Rhône-Alpes (France); Key Research Program of Frontier Sciences of CAS, CAS PIFI, CAS CCEPP, Fundamental Research Funds for the Central Universities, and Sci. & Tech. Program of Guangzhou (China); RFBR, RSF and Yandex LLC (Russia); GVA, XuntaGal and GENCAT (Spain); the Leverhulme Trust, the Royal Society and UKRI (United Kingdom).

A Correlation matrices

The correlation matrix for the statistical uncertainties is presented in Table 3 and the systematic uncertainty correlation matrix in Table 4.

Table 3: Correlation matrix for statistical uncertainties.

	$R^{KK\pi^0}$	$R^{\pi\pi\pi^0}$	$A_K^{K\pi\pi^0}$	$A_K^{KK\pi^0}$	$A_K^{\pi\pi\pi^0}$	$A_\pi^{KK\pi^0}$	$A_\pi^{\pi\pi\pi^0}$	R_K^+	R_K^-	R_π^+	R_π^-
$R^{KK\pi^0}$	1.00	0.05	−0.00	−0.01	−0.00	−0.00	0.00	0.02	0.01	0.00	0.00
$R^{\pi\pi\pi^0}$		1.00	−0.00	−0.00	−0.05	−0.00	0.00	0.02	0.01	−0.00	−0.00
$A_K^{K\pi\pi^0}$			1.00	0.01	0.02	0.04	0.08	−0.01	0.00	−0.01	0.01
$A_K^{KK\pi^0}$				1.00	0.00	−0.01	0.01	0.00	0.00	−0.00	0.00
$A_K^{\pi\pi\pi^0}$					1.00	0.01	−0.01	0.00	0.00	−0.00	0.00
$A_\pi^{KK\pi^0}$						1.00	0.04	−0.00	0.00	−0.00	0.00
$A_\pi^{\pi\pi\pi^0}$							1.00	−0.01	0.00	−0.01	0.01
R_K^+								1.00	0.09	−0.01	0.00
R_K^-									1.00	0.00	−0.01
R_π^+										1.00	0.01
R_π^-											1.00

Table 4: Correlation matrix for systematic uncertainties.

	$R^{KK\pi^0}$	$R^{\pi\pi\pi^0}$	$A_K^{K\pi\pi^0}$	$A_K^{KK\pi^0}$	$A_K^{\pi\pi\pi^0}$	$A_\pi^{KK\pi^0}$	$A_\pi^{\pi\pi\pi^0}$	R_K^+	R_K^-	R_π^+	R_π^-
$R^{KK\pi^0}$	1.00	0.83	−0.29	0.09	0.15	−0.23	−0.25	−0.10	−0.05	−0.15	−0.18
$R^{\pi\pi\pi^0}$		1.00	−0.39	−0.07	0.07	−0.26	−0.28	−0.22	−0.08	−0.15	−0.14
$A_K^{K\pi\pi^0}$			1.00	−0.06	−0.15	0.91	0.92	−0.04	−0.12	−0.09	−0.06
$A_K^{KK\pi^0}$				1.00	0.89	−0.20	−0.19	0.94	0.90	0.66	0.57
$A_K^{\pi\pi\pi^0}$					1.00	−0.23	−0.23	0.88	0.84	0.54	0.44
$A_\pi^{KK\pi^0}$						1.00	1.00	−0.18	−0.17	−0.05	−0.00
$A_\pi^{\pi\pi\pi^0}$							1.00	−0.17	−0.16	−0.06	−0.02
R_K^+								1.00	0.92	0.73	0.63
R_K^-									1.00	0.75	0.71
R_π^+										1.00	0.97
R_π^-											1.00

References

[1] J. Brod and J. Zupan, *The ultimate theoretical error on γ from $B \to DK$ decays*, JHEP **01** (2014) 051, arXiv:1308.5663.

[2] Heavy Flavor Averaging Group, Y. Amhis *et al.*, *Averages of b-hadron, c-hadron, and τ-lepton properties as of 2018*, Eur. Phys. J. **C81** (2021) 226, arXiv:1909.12524, updated results and plots available at https://hflav.web.cern.ch.

[3] CKMfitter group, J. Charles *et al.*, *CP violation and the CKM matrix: Assessing the impact of the asymmetric B factories*, Eur. Phys. J. **C41** (2005) 1, arXiv:hep-ph/0406184, updated results and plots available at http://ckmfitter.in2p3.fr/.

[4] M. Gronau and D. London, *How to determine all the angles of the unitarity triangle from $B^0 \to DK_S$ and $B_s^0 \to D\phi$*, Phys. Lett. **B253** (1991) 483.

[5] M. Gronau and D. Wyler, *On determining a weak phase from charged B decay asymmetries*, Phys. Lett. **B265** (1991) 172.

[6] D. Atwood, I. Dunietz, and A. Soni, *Enhanced CP violation with $B \to KD^0$ modes and extraction of the CKM angle gamma*, Phys. Rev. Lett. **78** (1997) 3257, arXiv:hep-ph/9612433.

[7] D. Atwood, I. Dunietz, and A. Soni, *Improved methods for observing CP violation in $B^\pm \to KD$ and measuring the CKM phase γ*, Phys. Rev. D **63** (2001) 036005.

[8] BaBar collaboration, J. P. Lees *et al.*, *Search for $b \to u$ Transitions in $B^\pm \to [K^\mp pi^\pm \pi^0]_D K^\pm$ Decays*, Phys. Rev. D **84** (2011) 012002, arXiv:1104.4472.

[9] Belle collaboration, M. Nayak *et al.*, *Evidence for the suppressed decay $B^- \to DK^-$, $D \to K^+\pi^-\pi^0$*, Phys. Rev. D **88** (2013) 091104, arXiv:1310.1741.

[10] LHCb collaboration, R. Aaij *et al.*, *A study of CP violation in $B^\mp \to Dh^\mp$ ($h = K, \pi$) with the modes $D \to K^\mp\pi^\pm\pi^0$, $D \to \pi^+\pi^-\pi^0$ and $D \to K^+K^-\pi^0$*, Phys. Rev. **D91** (2015) 112014, arXiv:1504.05442.

[11] S. Malde *et al.*, *First determination of the CP content of $D \to \pi^+\pi^-\pi^+\pi^-$ and updated determination of the CP contents of $D \to \pi^+\pi^-\pi^0$ and $D \to K^+K^-\pi^0$*, Phys. Lett. B **747** (2015) 9, arXiv:1504.05878.

[12] M. Nayak *et al.*, *First determination of the CP content of $D \to \pi^+\pi^-\pi^0$ and $D \to K^+K^-\pi^0$*, Phys. Lett. **B740** (2015) 1, arXiv:1410.3964.

[13] BESIII collaboration, M. Ablikim *et al.*, *Measurement of the $D \to K^-\pi^+\pi^+\pi^-$ and $D \to K^-\pi^+\pi^0$ coherence factors and average strong-phase differences in quantum-correlated $D\bar{D}$ decays*, JHEP **05** (2021) 164, arXiv:2103.05988.

[14] M. Rama, *Effect of $D - \overline{D}$ mixing in the extraction of γ with $B^- \to D^0K^-$ and $B^- \to D\pi^-$ decays*, Phys. Rev. **D89** (2014) 014021, arXiv:1307.4384.

[15] LHCb collaboration, A. A. Alves Jr. *et al.*, *The LHCb detector at the LHC*, JINST **3** (2008) S08005.

[16] LHCb collaboration, R. Aaij *et al.*, *LHCb detector performance*, Int. J. Mod. Phys. **A30** (2015) 1530022, arXiv:1412.6352.

[17] T. Sjöstrand, S. Mrenna, and P. Skands, *A brief introduction to PYTHIA 8.1*, Comput. Phys. Commun. **178** (2008) 852, arXiv:0710.3820.

[18] D. J. Lange, *The EvtGen particle decay simulation package*, Nucl. Instrum. Meth. **A462** (2001) 152.

[19] N. Davidson, T. Przedzinski, and Z. Was, *PHOTOS interface in C++: Technical and physics documentation*, Comp. Phys. Comm. **199** (2016) 86, arXiv:1011.0937.

[20] Geant4 collaboration, J. Allison *et al.*, *Geant4 developments and applications*, IEEE Trans. Nucl. Sci. **53** (2006) 270.

[21] M. Clemencic *et al.*, *The LHCb simulation application, Gauss: Design, evolution and experience*, J. Phys. Conf. Ser. **331** (2011) 032023.

[22] Particle Data Group, P. A. Zyla *et al.*, *Review of particle physics*, Prog. Theor. Exp. Phys. **2020** (2020) 083C01.

[23] W. D. Hulsbergen, *Decay chain fitting with a Kalman filter*, Nucl. Instrum. Meth. **A552** (2005) 566, arXiv:physics/0503191.

[24] L. Breiman, J. H. Friedman, R. A. Olshen, and C. J. Stone, *Classification and regression trees*, Wadsworth international group, Belmont, California, USA, 1984.

[25] Y. Freund and R. E. Schapire, *A decision-theoretic generalization of on-line learning and an application to boosting*, J. Comput. Syst. Sci. **55** (1997) 119.

[26] LHCb collaboration, R. Aaij *et al.*, *Measurement of CP observables in* $B^\pm \to D^{(*)}K^\pm$ *and* $B^\pm \to D^{(*)}\pi^\pm$ *decays*, Phys. Lett. **B777** (2018) 16, arXiv:1708.06370.

[27] LHCb collaboration, R. Aaij *et al.*, *Dalitz plot analysis of* $B^0_s \to \overline{D}^0 K^-\pi^+$ *decays*, Phys. Rev. **D90** (2014) 072003, arXiv:1407.7712.

[28] LHCb collaboration, R. Aaij *et al.*, *Measurement of the* $B^\pm$ *production asymmetry and the CP asymmetry in* $B^\pm \to J/\psi K^\pm$ *decays*, Phys. Rev. D **95** (2017) 052005, arXiv:1701.05501.

[29] J. Libby *et al.*, *New determination of the* $D^0 \to K^-\pi^+\pi^0$ *and* $D^0 \to K^-\pi^+\pi^-\pi^+$ *coherence factors and average strong-phase differences*, Phys. Lett. **B731** (2014) 197.

[30] T. Evans *et al.*, *Improved determination of the* $D \to K^-\pi^+\pi^+\pi^-$ *coherence factor and associated hadronic parameters from a combination of* $e^+e^- \to \psi(3770) \to c\bar{c}$ *and* $pp \to c\bar{c}X$ *data*, Phys. Lett. B **757** (2016) 520, arXiv:1602.07430, [Erratum: Phys.Lett.B 765, 402–403 (2017)].

[31] LHCb collaboration, R. Aaij *et al.*, *First observation of $D^0 - \overline{D}^0$ oscillations in $D^0 \to K^+\pi^+\pi^-\pi^-$ decays and a measurement of the associated coherence parameters*, Phys. Rev. Lett. **116** (2016) 241801, arXiv:1602.07224.

[32] S. S. Wilks, *The large-sample distribution of the likelihood ratio for testing composite hypotheses*, Ann. Math. Stat. **9** (1938) 60.

[33] LHCb collaboration, R. Aaij *et al.*, *Simultaneous determination of CKM angle γ and charm mixing parameters*, JHEP **12** (2021) 141, arXiv:2110.02350.

LHCb collaboration

R. Aaij[32], A.S.W. Abdelmotteleb[56], C. Abellán Beteta[50], F.J. Abudinen Gallego[56], T. Ackernley[60], B. Adeva[46], M. Adinolfi[54], H. Afsharnia[9], C. Agapopoulou[13], C.A. Aidala[87], S. Aiola[25], Z. Ajaltouni[9], S. Akar[65], J. Albrecht[15], F. Alessio[48], M. Alexander[59], A. Alfonso Albero[45], Z. Aliouche[62], G. Alkhazov[38], P. Alvarez Cartelle[55], S. Amato[2], J.L. Amey[54], Y. Amhis[11], L. An[48], L. Anderlini[22], N. Andersson[50], A. Andreianov[38], M. Andreotti[21], F. Archilli[17], A. Artamonov[44], M. Artuso[68], K. Arzymatov[42], E. Aslanides[10], M. Atzeni[50], B. Audurier[12], S. Bachmann[17], M. Bachmayer[49], J.J. Back[56], P. Baladron Rodriguez[46], V. Balagura[12], W. Baldini[21], J. Baptista Leite[1], M. Barbetti[22,h], R.J. Barlow[62], S. Barsuk[11], W. Barter[61], M. Bartolini[55], F. Baryshnikov[83], J.M. Basels[14], S. Bashir[34], G. Bassi[29], B. Batsukh[68], A. Battig[15], A. Bay[49], A. Beck[56], M. Becker[15], F. Bedeschi[29], I. Bediaga[1], A. Beiter[68], V. Belavin[42], S. Belin[27], V. Bellee[50], K. Belous[44], I. Belov[40], I. Belyaev[41], G. Bencivenni[23], E. Ben-Haim[13], A. Berezhnoy[40], R. Bernet[50], D. Berninghoff[17], H.C. Bernstein[68], C. Bertella[48], A. Bertolin[28], C. Betancourt[50], F. Betti[48], Ia. Bezshyiko[50], S. Bhasin[54], J. Bhom[35], L. Bian[73], M.S. Bieker[15], N.V. Biesuz[21], S. Bifani[53], P. Billoir[13], A. Biolchini[32], M. Birch[61], F.C.R. Bishop[55], A. Bitadze[62], A. Bizzeti[22,l], M. Bjørn[63], M.P. Blago[48], T. Blake[56], F. Blanc[49], S. Blusk[68], D. Bobulska[59], J.A. Boelhauve[15], O. Boente Garcia[46], T. Boettcher[65], A. Boldyrev[82], A. Bondar[43], N. Bondar[38,48], S. Borghi[62], M. Borisyak[42], M. Borsato[17], J.T. Borsuk[35], S.A. Bouchiba[49], T.J.V. Bowcock[60,48], A. Boyer[48], C. Bozzi[21], M.J. Bradley[61], S. Braun[66], A. Brea Rodriguez[46], J. Brodzicka[35], A. Brossa Gonzalo[56], D. Brundu[27], A. Buonaura[50], L. Buonincontri[28], A.T. Burke[62], C. Burr[48], A. Bursche[72], A. Butkevich[39], J.S. Butter[32], J. Buytaert[48], W. Byczynski[48], S. Cadeddu[27], H. Cai[73], R. Calabrese[21,g], L. Calefice[15,13], S. Cali[23], R. Calladine[53], M. Calvi[26,k], M. Calvo Gomez[85], P. Camargo Magalhaes[54], P. Campana[23], A.F. Campoverde Quezada[6], S. Capelli[26,k], L. Capriotti[20,e], A. Carbone[20,e], G. Carboni[31,q], R. Cardinale[24,i], A. Cardini[27], I. Carli[4], P. Carniti[26,k], L. Carus[14], K. Carvalho Akiba[32], A. Casais Vidal[46], R. Caspary[17], G. Casse[60], M. Cattaneo[48], G. Cavallero[48], S. Celani[49], J. Cerasoli[10], D. Cervenkov[63], A.J. Chadwick[60], M.G. Chapman[54], M. Charles[13], Ph. Charpentier[48], G. Chatzikonstantinidis[53], C.A. Chavez Barajas[60], M. Chefdeville[8], C. Chen[3], S. Chen[4], A. Chernov[35], V. Chobanova[46], S. Cholak[49], M. Chrzaszcz[35], A. Chubykin[38], V. Chulikov[38], P. Ciambrone[23], M.F. Cicala[56], X. Cid Vidal[46], G. Ciezarek[48], P.E.L. Clarke[58], M. Clemencic[48], H.V. Cliff[55], J. Closier[48], J.L. Cobbledick[62], V. Coco[48], J.A.B. Coelho[11], J. Cogan[10], E. Cogneras[9], L. Cojocariu[37], P. Collins[48], T. Colombo[48], L. Congedo[19,d], A. Contu[27], N. Cooke[53], G. Coombs[59], I. Corredoira [46], G. Corti[48], C.M. Costa Sobral[56], B. Couturier[48], D.C. Craik[64], J. Crkovská[67], M. Cruz Torres[1], R. Currie[58], C.L. Da Silva[67], S. Dadabaev[83], L. Dai[71], E. Dall'Occo[15], J. Dalseno[46], C. D'Ambrosio[48], A. Danilina[41], P. d'Argent[48], A. Dashkina[83], J.E. Davies[62], A. Davis[62], O. De Aguiar Francisco[62], K. De Bruyn[79], S. De Capua[62], M. De Cian[49], E. De Lucia[23], J.M. De Miranda[1], L. De Paula[2], M. De Serio[19,d], D. De Simone[50], P. De Simone[23], F. De Vellis[15], J.A. de Vries[80], C.T. Dean[67], F. Debernardis[19,d], D. Decamp[8], V. Dedu[10], L. Del Buono[13], B. Delaney[55], H.-P. Dembinski[15], A. Dendek[34], V. Denysenko[50], D. Derkach[82], O. Deschamps[9], F. Desse[11], F. Dettori[27,f], B. Dey[77], A. Di Cicco[23], P. Di Nezza[23], S. Didenko[83], L. Dieste Maronas[46], H. Dijkstra[48], V. Dobishuk[52], C. Dong[3], A.M. Donohoe[18], F. Dordei[27], A.C. dos Reis[1], L. Douglas[59], A. Dovbnya[51], A.G. Downes[8], M.W. Dudek[35], L. Dufour[48], V. Duk[78], P. Durante[48], J.M. Durham[67], D. Dutta[62], A. Dziurda[35], A. Dzyuba[38], S. Easo[57], U. Egede[69], V. Egorychev[41], S. Eidelman[43,v,†], S. Eisenhardt[58], S. Ek-In[49], L. Eklund[86], S. Ely[68], A. Ene[37], E. Epple[67], S. Escher[14], J. Eschle[50], S. Esen[50], T. Evans[48], L.N. Falcao[1], Y. Fan[6], B. Fang[73], S. Farry[60], D. Fazzini[26,k], M. Féo[48], A. Fernandez Prieto[46], A.D. Fernez[66], F. Ferrari[20,e], L. Ferreira Lopes[49], F. Ferreira Rodrigues[2], S. Ferreres Sole[32], M. Ferrillo[50], M. Ferro-Luzzi[48], S. Filippov[39], R.A. Fini[19], M. Fiorini[21,g],

M. Firlej[34], K.M. Fischer[63], D.S. Fitzgerald[87], C. Fitzpatrick[62], T. Fiutowski[34], A. Fkiaras[48], F. Fleuret[12], M. Fontana[13], F. Fontanelli[24,i], R. Forty[48], D. Foulds-Holt[55], V. Franco Lima[60], M. Franco Sevilla[66], M. Frank[48], E. Franzoso[21], G. Frau[17], C. Frei[48], D.A. Friday[59], J. Fu[6], Q. Fuehring[15], E. Gabriel[32], G. Galati[19,d], A. Gallas Torreira[46], D. Galli[20,e], S. Gambetta[58,48], Y. Gan[3], M. Gandelman[2], P. Gandini[25], Y. Gao[5], M. Garau[27], L.M. Garcia Martin[56], P. Garcia Moreno[45], J. García Pardiñas[26,k], B. Garcia Plana[46], F.A. Garcia Rosales[12], L. Garrido[45], C. Gaspar[48], R.E. Geertsema[32], D. Gerick[17], L.L. Gerken[15], E. Gersabeck[62], M. Gersabeck[62], T. Gershon[56], D. Gerstel[10], L. Giambastiani[28], V. Gibson[55], H.K. Giemza[36], A.L. Gilman[63], M. Giovannetti[23,q], A. Gioventù[46], P. Gironella Gironell[45], C. Giugliano[21,g], K. Gizdov[58], E.L. Gkougkousis[48], V.V. Gligorov[13], C. Göbel[70], E. Golobardes[85], D. Golubkov[41], A. Golutvin[61,83], A. Gomes[1,a], S. Gomez Fernandez[45], F. Goncalves Abrantes[63], M. Goncerz[35], G. Gong[3], P. Gorbounov[41], I.V. Gorelov[40], C. Gotti[26], E. Govorkova[48], J.P. Grabowski[17], T. Grammatico[13], L.A. Granado Cardoso[48], E. Graugés[45], E. Graverini[49], G. Graziani[22], A. Grecu[37], L.M. Greeven[32], N.A. Grieser[4], L. Grillo[62], S. Gromov[83], B.R. Gruberg Cazon[63], C. Gu[3], M. Guarise[21], M. Guittiere[11], P. A. Günther[17], E. Gushchin[39], A. Guth[14], Y. Guz[44], T. Gys[48], T. Hadavizadeh[69], G. Haefeli[49], C. Haen[48], J. Haimberger[48], T. Halewood-leagas[60], P.M. Hamilton[66], J.P. Hammerich[60], Q. Han[7], X. Han[17], T.H. Hancock[63], E.B. Hansen[62], S. Hansmann-Menzemer[17], N. Harnew[63], T. Harrison[60], C. Hasse[48], M. Hatch[48], J. He[6,b], M. Hecker[61], K. Heijhoff[32], K. Heinicke[15], R.D.L. Henderson[69], A.M. Hennequin[48], K. Hennessy[60], L. Henry[48], J. Heuel[14], A. Hicheur[2], D. Hill[49], M. Hilton[62], S.E. Hollitt[15], R. Hou[7], Y. Hou[8], J. Hu[17], J. Hu[72], W. Hu[7], X. Hu[3], W. Huang[6], X. Huang[73], W. Hulsbergen[32], R.J. Hunter[56], M. Hushchyn[82], D. Hutchcroft[60], D. Hynds[32], P. Ibis[15], M. Idzik[34], D. Ilin[38], P. Ilten[65], A. Inglessi[38], A. Ishteev[83], K. Ivshin[38], R. Jacobsson[48], H. Jage[14], S. Jakobsen[48], E. Jans[32], B.K. Jashal[47], A. Jawahery[66], V. Jevtic[15], X. Jiang[4], M. John[63], D. Johnson[64], C.R. Jones[55], T.P. Jones[56], B. Jost[48], N. Jurik[48], S.H. Kalavan Kadavath[34], S. Kandybei[51], Y. Kang[3], M. Karacson[48], M. Karpov[82], J.W. Kautz[65], F. Keizer[48], D.M. Keller[68], M. Kenzie[56], T. Ketel[33], B. Khanji[15], A. Kharisova[84], S. Kholodenko[44], T. Kirn[14], V.S. Kirsebom[49], O. Kitouni[64], S. Klaver[32], N. Kleijne[29], K. Klimaszewski[36], M.R. Kmiec[36], S. Koliiev[52], A. Kondybayeva[83], A. Konoplyannikov[41], P. Kopciewicz[34], R. Kopecna[17], P. Koppenburg[32], M. Korolev[40], I. Kostiuk[32,52], O. Kot[52], S. Kotriakhova[21,38], P. Kravchenko[38], L. Kravchuk[39], R.D. Krawczyk[48], M. Kreps[56], F. Kress[61], S. Kretzschmar[14], P. Krokovny[43,v], W. Krupa[34], W. Krzemien[36], J. Kubat[17], M. Kucharczyk[35], V. Kudryavtsev[43,v], H.S. Kuindersma[32,33], G.J. Kunde[67], T. Kvaratskheliya[41], D. Lacarrere[48], G. Lafferty[62], A. Lai[27], A. Lampis[27], D. Lancierini[50], J.J. Lane[62], R. Lane[54], G. Lanfranchi[23], C. Langenbruch[14], J. Langer[15], O. Lantwin[83], T. Latham[56], F. Lazzari[29,r], R. Le Gac[10], S.H. Lee[87], R. Lefèvre[9], A. Leflat[40], S. Legotin[83], O. Leroy[10], T. Lesiak[35], B. Leverington[17], H. Li[72], P. Li[17], S. Li[7], Y. Li[4], Y. Li[4], Z. Li[68], X. Liang[68], T. Lin[61], R. Lindner[48], V. Lisovskyi[15], R. Litvinov[27], G. Liu[72], H. Liu[6], Q. Liu[6], S. Liu[4], A. Lobo Salvia[45], A. Loi[27], J. Lomba Castro[46], I. Longstaff[59], J.H. Lopes[2], S. Lopez Solino[46], G.H. Lovell[55], Y. Lu[4], C. Lucarelli[22,h], D. Lucchesi[28,m], S. Luchuk[39], M. Lucio Martinez[32], V. Lukashenko[32,52], Y. Luo[3], A. Lupato[62], E. Luppi[21,g], O. Lupton[56], A. Lusiani[29,n], X. Lyu[6], L. Ma[4], R. Ma[6], S. Maccolini[20,e], F. Machefert[11], F. Maciuc[37], V. Macko[49], P. Mackowiak[15], S. Maddrell-Mander[54], O. Madejczyk[34], L.R. Madhan Mohan[54], O. Maev[38], A. Maevskiy[82], M.W. Majewski[34], J.J. Malczewski[35], S. Malde[63], B. Malecki[48], A. Malinin[81], T. Maltsev[43,v], H. Malygina[17], G. Manca[27,f], G. Mancinelli[10], D. Manuzzi[20,e], D. Marangotto[25,j], J. Maratas[9,t], J.F. Marchand[8], U. Marconi[20], S. Mariani[22,h], C. Marin Benito[48], M. Marinangeli[49], J. Marks[17], A.M. Marshall[54], P.J. Marshall[60], G. Martelli[78], G. Martellotti[30], L. Martinazzoli[48,k], M. Martinelli[26,k], D. Martinez Santos[46], F. Martinez Vidal[47], A. Massafferri[1], M. Materok[14], R. Matev[48], A. Mathad[50], V. Matiunin[41], C. Matteuzzi[26], K.R. Mattioli[87], A. Mauri[32], E. Maurice[12], J. Mauricio[45], M. Mazurek[48], M. McCann[61], L. Mcconnell[18], T.H. Mcgrath[62],

N.T. Mchugh[59], A. McNab[62], R. McNulty[18], J.V. Mead[60], B. Meadows[65], G. Meier[15], D. Melnychuk[36], S. Meloni[26,k], M. Merk[32,80], A. Merli[25,j], L. Meyer Garcia[2], M. Mikhasenko[75,c], D.A. Milanes[74], E. Millard[56], M. Milovanovic[48], M.-N. Minard[8], A. Minotti[26,k], L. Minzoni[21,g], S.E. Mitchell[58], B. Mitreska[62], D.S. Mitzel[15], A. Mödden [15], R.A. Mohammed[63], R.D. Moise[61], S. Mokhnenko[82], T. Mombächer[46], I.A. Monroy[74], S. Monteil[9], M. Morandin[28], G. Morello[23], M.J. Morello[29,n], J. Moron[34], A.B. Morris[75], A.G. Morris[56], R. Mountain[68], H. Mu[3], F. Muheim[58,48], M. Mulder[79], D. Müller[48], K. Müller[50], C.H. Murphy[63], D. Murray[62], R. Murta[61], P. Muzzetto[27], P. Naik[54], T. Nakada[49], R. Nandakumar[57], T. Nanut[48], I. Nasteva[2], M. Needham[58], N. Neri[25,j], S. Neubert[75], N. Neufeld[48], R. Newcombe[61], E.M. Niel[11], S. Nieswand[14], N. Nikitin[40], N.S. Nolte[64], C. Normand[8], C. Nunez[87], A. Oblakowska-Mucha[34], V. Obraztsov[44], T. Oeser[14], D.P. O'Hanlon[54], S. Okamura[21], R. Oldeman[27,f], F. Oliva[58], M.E. Olivares[68], C.J.G. Onderwater[79], R.H. O'Neil[58], J.M. Otalora Goicochea[2], T. Ovsiannikova[41], P. Owen[50], A. Oyanguren[47], K.O. Padeken[75], B. Pagare[56], P.R. Pais[48], T. Pajero[63], A. Palano[19], M. Palutan[23], Y. Pan[62], G. Panshin[84], A. Papanestis[57], M. Pappagallo[19,d], L.L. Pappalardo[21,g], C. Pappenheimer[65], W. Parker[66], C. Parkes[62], B. Passalacqua[21], G. Passaleva[22], A. Pastore[19], M. Patel[61], C. Patrignani[20,e], C.J. Pawley[80], A. Pearce[48,57], A. Pellegrino[32], M. Pepe Altarelli[48], S. Perazzini[20], D. Pereima[41], A. Pereiro Castro[46], P. Perret[9], M. Petric[59,48], K. Petridis[54], A. Petrolini[24,i], A. Petrov[81], S. Petrucci[58], M. Petruzzo[25], T.T.H. Pham[68], A. Philippov[42], R. Piandani[6], L. Pica[29,n], M. Piccini[78], B. Pietrzyk[8], G. Pietrzyk[49], M. Pili[63], D. Pinci[30], F. Pisani[48], M. Pizzichemi[26,48,k], Resmi P.K[10], V. Placinta[37], J. Plews[53], M. Plo Casasus[46], F. Polci[13], M. Poli Lener[23], M. Poliakova[68], A. Poluektov[10], N. Polukhina[83,u], I. Polyakov[68], E. Polycarpo[2], S. Ponce[48], D. Popov[6,48], S. Popov[42], S. Poslavskii[44], K. Prasanth[35], L. Promberger[48], C. Prouve[46], V. Pugatch[52], V. Puill[11], H. Pullen[63], G. Punzi[29,o], H. Qi[3], W. Qian[6], N. Qin[3], R. Quagliani[49], N.V. Raab[18], R.I. Rabadan Trejo[6], B. Rachwal[34], J.H. Rademacker[54], M. Rama[29], M. Ramos Pernas[56], M.S. Rangel[2], F. Ratnikov[42,82], G. Raven[33], M. Reboud[8], F. Redi[49], F. Reiss[62], C. Remon Alepuz[47], Z. Ren[3], V. Renaudin[63], R. Ribatti[29], S. Ricciardi[57], K. Rinnert[60], P. Robbe[11], G. Robertson[58], A.B. Rodrigues[49], E. Rodrigues[60], J.A. Rodriguez Lopez[74], E.R.R. Rodriguez Rodriguez[46], A. Rollings[63], P. Roloff[48], V. Romanovskiy[44], M. Romero Lamas[46], A. Romero Vidal[46], J.D. Roth[87,†], M. Rotondo[23], M.S. Rudolph[68], T. Ruf[48], R.A. Ruiz Fernandez[46], J. Ruiz Vidal[47], A. Ryzhikov[82], J. Ryzka[34], J.J. Saborido Silva[46], N. Sagidova[38], N. Sahoo[56], B. Saitta[27,f], M. Salomoni[48], C. Sanchez Gras[32], R. Santacesaria[30], C. Santamarina Rios[46], M. Santimaria[23], E. Santovetti[31,q], D. Saranin[83], G. Sarpis[14], M. Sarpis[75], A. Sarti[30], C. Satriano[30,p], A. Satta[31], M. Saur[15], D. Savrina[41,40], H. Sazak[9], L.G. Scantlebury Smead[63], A. Scarabotto[13], S. Schael[14], S. Scherl[60], M. Schiller[59], H. Schindler[48], M. Schmelling[16], B. Schmidt[48], S. Schmitt[14], O. Schneider[49], A. Schopper[48], M. Schubiger[32], S. Schulte[49], M.H. Schune[11], R. Schwemmer[48], B. Sciascia[23,48], S. Sellam[46], A. Semennikov[41], M. Senghi Soares[33], A. Sergi[24,i], N. Serra[50], L. Sestini[28], A. Seuthe[15], Y. Shang[5], D.M. Shangase[87], M. Shapkin[44], I. Shchemerov[83], L. Shchutska[49], T. Shears[60], L. Shekhtman[43,v], Z. Shen[5], S. Sheng[4], V. Shevchenko[81], E.B. Shields[26,k], Y. Shimizu[11], E. Shmanin[83], J.D. Shupperd[68], B.G. Siddi[21], R. Silva Coutinho[50], G. Simi[28], S. Simone[19,d], N. Skidmore[62], T. Skwarnicki[68], M.W. Slater[53], I. Slazyk[21,g], J.C. Smallwood[63], J.G. Smeaton[55], A. Smetkina[41], E. Smith[50], M. Smith[61], A. Snoch[32], L. Soares Lavra[9], M.D. Sokoloff[65], F.J.P. Soler[59], A. Solovev[38], I. Solovyev[38], F.L. Souza De Almeida[2], B. Souza De Paula[2], B. Spaan[15,†], E. Spadaro Norella[25,j], P. Spradlin[59], F. Stagni[48], M. Stahl[65], S. Stahl[48], S. Stanislaus[63], O. Steinkamp[50,83], O. Stenyakin[44], H. Stevens[15], S. Stone[68,†], D. Strekalina[83], F. Suljik[63], J. Sun[27], L. Sun[73], Y. Sun[66], P. Svihra[62], P.N. Swallow[53], K. Swientek[34], A. Szabelski[36], T. Szumlak[34], M. Szymanski[48], S. Taneja[62], A.R. Tanner[54], M.D. Tat[63], A. Terentev[83], F. Teubert[48], E. Thomas[48], D.J.D. Thompson[53], K.A. Thomson[60], H. Tilquin[61], V. Tisserand[9], S. T'Jampens[8], M. Tobin[4], L. Tomassetti[21,g], X. Tong[5],

D. Torres Machado[1], D.Y. Tou[13], E. Trifonova[83], S.M. Trilov[54], C. Trippl[49], G. Tuci[6], A. Tully[49], N. Tuning[32,48], A. Ukleja[36,48], D.J. Unverzagt[17], E. Ursov[83], A. Usachov[32], A. Ustyuzhanin[42,82], U. Uwer[17], A. Vagner[84], V. Vagnoni[20], A. Valassi[48], G. Valenti[20], N. Valls Canudas[85], M. van Beuzekom[32], M. Van Dijk[49], H. Van Hecke[67], E. van Herwijnen[83], M. van Veghel[79], R. Vazquez Gomez[45], P. Vazquez Regueiro[46], C. Vázquez Sierra[48], S. Vecchi[21], J.J. Velthuis[54], M. Veltri[22,s], A. Venkateswaran[68], M. Veronesi[32], M. Vesterinen[56], D. Vieira[65], M. Vieites Diaz[49], H. Viemann[76], X. Vilasis-Cardona[85], E. Vilella Figueras[60], A. Villa[20], P. Vincent[13], F.C. Volle[11], D. Vom Bruch[10], A. Vorobyev[38,†], V. Vorobyev[43,v], N. Voropaev[38], K. Vos[80], R. Waldi[17], J. Walsh[29], C. Wang[17], J. Wang[5], J. Wang[4], J. Wang[3], J. Wang[73], M. Wang[3], R. Wang[54], Y. Wang[7], Z. Wang[50], Z. Wang[3], Z. Wang[6], J.A. Ward[56], N.K. Watson[53], S.G. Weber[13], D. Websdale[61], C. Weisser[64], B.D.C. Westhenry[54], D.J. White[62], M. Whitehead[54], A.R. Wiederhold[56], D. Wiedner[15], G. Wilkinson[63], M. Wilkinson[68], I. Williams[55], M. Williams[64], M.R.J. Williams[58], F.F. Wilson[57], W. Wislicki[36], M. Witek[35], L. Witola[17], G. Wormser[11], S.A. Wotton[55], H. Wu[68], K. Wyllie[48], Z. Xiang[6], D. Xiao[7], Y. Xie[7], A. Xu[5], J. Xu[6], L. Xu[3], M. Xu[7], Q. Xu[6], Z. Xu[5], Z. Xu[6], D. Yang[3], S. Yang[6], Y. Yang[6], Z. Yang[5], Z. Yang[66], Y. Yao[68], L.E. Yeomans[60], H. Yin[7], J. Yu[71], X. Yuan[68], O. Yushchenko[44], E. Zaffaroni[49], M. Zavertyaev[16,u], M. Zdybal[35], O. Zenaiev[48], M. Zeng[3], D. Zhang[7], L. Zhang[3], S. Zhang[71], S. Zhang[5], Y. Zhang[5], Y. Zhang[63], A. Zharkova[83], A. Zhelezov[17], Y. Zheng[6], T. Zhou[5], X. Zhou[6], Y. Zhou[6], V. Zhovkovska[11], X. Zhu[3], X. Zhu[7], Z. Zhu[6], V. Zhukov[14,40], J.B. Zonneveld[58], Q. Zou[4], S. Zucchelli[20,e], D. Zuliani[28], G. Zunica[62].

[1] *Centro Brasileiro de Pesquisas Físicas (CBPF), Rio de Janeiro, Brazil*
[2] *Universidade Federal do Rio de Janeiro (UFRJ), Rio de Janeiro, Brazil*
[3] *Center for High Energy Physics, Tsinghua University, Beijing, China*
[4] *Institute Of High Energy Physics (IHEP), Beijing, China*
[5] *School of Physics State Key Laboratory of Nuclear Physics and Technology, Peking University, Beijing, China*
[6] *University of Chinese Academy of Sciences, Beijing, China*
[7] *Institute of Particle Physics, Central China Normal University, Wuhan, Hubei, China*
[8] *Univ. Savoie Mont Blanc, CNRS, IN2P3-LAPP, Annecy, France*
[9] *Université Clermont Auvergne, CNRS/IN2P3, LPC, Clermont-Ferrand, France*
[10] *Aix Marseille Univ, CNRS/IN2P3, CPPM, Marseille, France*
[11] *Université Paris-Saclay, CNRS/IN2P3, IJCLab, Orsay, France*
[12] *Laboratoire Leprince-Ringuet, CNRS/IN2P3, Ecole Polytechnique, Institut Polytechnique de Paris, Palaiseau, France*
[13] *LPNHE, Sorbonne Université, Paris Diderot Sorbonne Paris Cité, CNRS/IN2P3, Paris, France*
[14] *I. Physikalisches Institut, RWTH Aachen University, Aachen, Germany*
[15] *Fakultät Physik, Technische Universität Dortmund, Dortmund, Germany*
[16] *Max-Planck-Institut für Kernphysik (MPIK), Heidelberg, Germany*
[17] *Physikalisches Institut, Ruprecht-Karls-Universität Heidelberg, Heidelberg, Germany*
[18] *School of Physics, University College Dublin, Dublin, Ireland*
[19] *INFN Sezione di Bari, Bari, Italy*
[20] *INFN Sezione di Bologna, Bologna, Italy*
[21] *INFN Sezione di Ferrara, Ferrara, Italy*
[22] *INFN Sezione di Firenze, Firenze, Italy*
[23] *INFN Laboratori Nazionali di Frascati, Frascati, Italy*
[24] *INFN Sezione di Genova, Genova, Italy*
[25] *INFN Sezione di Milano, Milano, Italy*
[26] *INFN Sezione di Milano-Bicocca, Milano, Italy*
[27] *INFN Sezione di Cagliari, Monserrato, Italy*
[28] *Universita degli Studi di Padova, Universita e INFN, Padova, Padova, Italy*
[29] *INFN Sezione di Pisa, Pisa, Italy*
[30] *INFN Sezione di Roma La Sapienza, Roma, Italy*
[31] *INFN Sezione di Roma Tor Vergata, Roma, Italy*

[32] *Nikhef National Institute for Subatomic Physics, Amsterdam, Netherlands*
[33] *Nikhef National Institute for Subatomic Physics and VU University Amsterdam, Amsterdam, Netherlands*
[34] *AGH - University of Science and Technology, Faculty of Physics and Applied Computer Science, Kraków, Poland*
[35] *Henryk Niewodniczanski Institute of Nuclear Physics Polish Academy of Sciences, Kraków, Poland*
[36] *National Center for Nuclear Research (NCBJ), Warsaw, Poland*
[37] *Horia Hulubei National Institute of Physics and Nuclear Engineering, Bucharest-Magurele, Romania*
[38] *Petersburg Nuclear Physics Institute NRC Kurchatov Institute (PNPI NRC KI), Gatchina, Russia*
[39] *Institute for Nuclear Research of the Russian Academy of Sciences (INR RAS), Moscow, Russia*
[40] *Institute of Nuclear Physics, Moscow State University (SINP MSU), Moscow, Russia*
[41] *Institute of Theoretical and Experimental Physics NRC Kurchatov Institute (ITEP NRC KI), Moscow, Russia*
[42] *Yandex School of Data Analysis, Moscow, Russia*
[43] *Budker Institute of Nuclear Physics (SB RAS), Novosibirsk, Russia*
[44] *Institute for High Energy Physics NRC Kurchatov Institute (IHEP NRC KI), Protvino, Russia, Protvino, Russia*
[45] *ICCUB, Universitat de Barcelona, Barcelona, Spain*
[46] *Instituto Galego de Física de Altas Enerxías (IGFAE), Universidade de Santiago de Compostela, Santiago de Compostela, Spain*
[47] *Instituto de Fisica Corpuscular, Centro Mixto Universidad de Valencia - CSIC, Valencia, Spain*
[48] *European Organization for Nuclear Research (CERN), Geneva, Switzerland*
[49] *Institute of Physics, Ecole Polytechnique Fédérale de Lausanne (EPFL), Lausanne, Switzerland*
[50] *Physik-Institut, Universität Zürich, Zürich, Switzerland*
[51] *NSC Kharkiv Institute of Physics and Technology (NSC KIPT), Kharkiv, Ukraine*
[52] *Institute for Nuclear Research of the National Academy of Sciences (KINR), Kyiv, Ukraine*
[53] *University of Birmingham, Birmingham, United Kingdom*
[54] *H.H. Wills Physics Laboratory, University of Bristol, Bristol, United Kingdom*
[55] *Cavendish Laboratory, University of Cambridge, Cambridge, United Kingdom*
[56] *Department of Physics, University of Warwick, Coventry, United Kingdom*
[57] *STFC Rutherford Appleton Laboratory, Didcot, United Kingdom*
[58] *School of Physics and Astronomy, University of Edinburgh, Edinburgh, United Kingdom*
[59] *School of Physics and Astronomy, University of Glasgow, Glasgow, United Kingdom*
[60] *Oliver Lodge Laboratory, University of Liverpool, Liverpool, United Kingdom*
[61] *Imperial College London, London, United Kingdom*
[62] *Department of Physics and Astronomy, University of Manchester, Manchester, United Kingdom*
[63] *Department of Physics, University of Oxford, Oxford, United Kingdom*
[64] *Massachusetts Institute of Technology, Cambridge, MA, United States*
[65] *University of Cincinnati, Cincinnati, OH, United States*
[66] *University of Maryland, College Park, MD, United States*
[67] *Los Alamos National Laboratory (LANL), Los Alamos, United States*
[68] *Syracuse University, Syracuse, NY, United States*
[69] *School of Physics and Astronomy, Monash University, Melbourne, Australia, associated to* [56]
[70] *Pontifícia Universidade Católica do Rio de Janeiro (PUC-Rio), Rio de Janeiro, Brazil, associated to* [2]
[71] *Physics and Micro Electronic College, Hunan University, Changsha City, China, associated to* [7]
[72] *Guangdong Provincial Key Laboratory of Nuclear Science, Guangdong-Hong Kong Joint Laboratory of Quantum Matter, Institute of Quantum Matter, South China Normal University, Guangzhou, China, associated to* [3]
[73] *School of Physics and Technology, Wuhan University, Wuhan, China, associated to* [3]
[74] *Departamento de Fisica , Universidad Nacional de Colombia, Bogota, Colombia, associated to* [13]
[75] *Universität Bonn - Helmholtz-Institut für Strahlen und Kernphysik, Bonn, Germany, associated to* [17]
[76] *Institut für Physik, Universität Rostock, Rostock, Germany, associated to* [17]
[77] *Eotvos Lorand University, Budapest, Hungary, associated to* [48]
[78] *INFN Sezione di Perugia, Perugia, Italy, associated to* [21]
[79] *Van Swinderen Institute, University of Groningen, Groningen, Netherlands, associated to* [32]
[80] *Universiteit Maastricht, Maastricht, Netherlands, associated to* [32]

[81] *National Research Centre Kurchatov Institute, Moscow, Russia, associated to* [41]
[82] *National Research University Higher School of Economics, Moscow, Russia, associated to* [42]
[83] *National University of Science and Technology "MISIS", Moscow, Russia, associated to* [41]
[84] *National Research Tomsk Polytechnic University, Tomsk, Russia, associated to* [41]
[85] *DS4DS, La Salle, Universitat Ramon Llull, Barcelona, Spain, associated to* [45]
[86] *Department of Physics and Astronomy, Uppsala University, Uppsala, Sweden, associated to* [59]
[87] *University of Michigan, Ann Arbor, United States, associated to* [68]

[a] *Universidade Federal do Triângulo Mineiro (UFTM), Uberaba-MG, Brazil*
[b] *Hangzhou Institute for Advanced Study, UCAS, Hangzhou, China*
[c] *Excellence Cluster ORIGINS, Munich, Germany*
[d] *Università di Bari, Bari, Italy*
[e] *Università di Bologna, Bologna, Italy*
[f] *Università di Cagliari, Cagliari, Italy*
[g] *Università di Ferrara, Ferrara, Italy*
[h] *Università di Firenze, Firenze, Italy*
[i] *Università di Genova, Genova, Italy*
[j] *Università degli Studi di Milano, Milano, Italy*
[k] *Università di Milano Bicocca, Milano, Italy*
[l] *Università di Modena e Reggio Emilia, Modena, Italy*
[m] *Università di Padova, Padova, Italy*
[n] *Scuola Normale Superiore, Pisa, Italy*
[o] *Università di Pisa, Pisa, Italy*
[p] *Università della Basilicata, Potenza, Italy*
[q] *Università di Roma Tor Vergata, Roma, Italy*
[r] *Università di Siena, Siena, Italy*
[s] *Università di Urbino, Urbino, Italy*
[t] *MSU - Iligan Institute of Technology (MSU-IIT), Iligan, Philippines*
[u] *P.N. Lebedev Physical Institute, Russian Academy of Science (LPI RAS), Moscow, Russia*
[v] *Novosibirsk State University, Novosibirsk, Russia*

[†] *Deceased*